

Magneto-electronic effects in pyrochlore $Tl_2Mn_2O_7$: Role of Tl-O covalency

David J. Singh

Complex Systems Theory Branch, Naval Research Laboratory, Washington, DC 20375

(Received 12 August 1996)

First principles calculations are used to elucidate the magnetic and electronic structure of pyrochlore $Tl_2Mn_2O_7$. It is found that the bonding has an important covalent contribution from Tl-O interactions. The high spin ferromagnetic ground state has a very large differentiation between minority and majority spin electronic properties. In particular, the minority spin channel contains a single, nearly spherical high velocity Fermi surface derived from strongly mixed combinations of Tl, Mn, and O orbitals, while the majority spin channel contains three smaller Fermi surfaces with much lower Fermi velocities. The proximity to a band edge in the majority channel may lead to localization of these states if sufficient disorder is present. In any case, highly spin differentiated transport results, with the conduction dominated by the minority channel. [S0163-1829(97)03801-0]

INTRODUCTION

There has been a recent revival of interest in perovskite structure Mn oxides due to the discovery of colossal magnetoresistance (CMR) effects in $La_{1-x}D_xMnO_3$, where D is a divalent cation, e.g., Ca.^{1,2} In the regime near $x=1/3$, where large CMR effects occur, these manganates have ferromagnetic ground states and are in a nearly cubic perovskite structure. The high spin Mn ions have nominally full majority spin t_{2g} orbitals while the majority spin e_g orbitals have a fractional occupation depending on x . As was recognized early on,³⁻⁵ these alloys display strong couplings between the doping level (x), magnetic order, structure, and transport. Understanding these is likely crucial for formulating a satisfactory theory of the CMR effect.

Zener⁶ identified a mechanism, known as double exchange (DEX), that can qualitatively account for the relationship between magnetic order, doping, and transport. In this picture, both ferromagnetism and metallic conduction are stabilized by a partial occupation of a Mn majority spin e_g orbital. When only Mn^{4+} ions are present, such as in $CaMnO_3$, there is no partial occupation of a Mn e_g orbital and there are no ferromagnetic interactions in the DEX model. Doping is essential for ferromagnetism and conduction in the DEX framework.

The qualitative predictions of the DEX model are also found in first principles calculations based on density functional theory.⁷⁻¹¹ Such calculations have shown that the local spin density approximation (LSDA) can reliably describe the electronic, magnetic, and structural properties of these manganese perovskites. $CaMnO_3$ is predicted to be an antiferromagnetic insulator in its ground state. $LaMnO_3$ is also found to be an antiferromagnetic insulator in accord with the DEX model, while intermediate compositions are found to be ferromagnetic metals. However, $LaMnO_3$ in the cubic perovskite structure is found to be a ferromagnetic metal with strongly hybridized (Mn $3d$ -O $2p$) majority spin bands around the Fermi energy, E_F , while the insulating ground state occurs only when the distortion from the cubic perovskite structure is included. The strongly hybridized electronic structure found in LSDA calculations is beyond the scope of

the DEX model, which is based on Hund's rule ions. Although it is recognized that the DEX model is qualitative, much discussion of the CMR manganates is based on it and its extensions.

The discovery of a CMR effect in pyrochlore structure $Tl_2Mn_2O_7$ (Refs. 12 and 13) is of interest because this material does not fit within the DEX framework. In this pyrochlore structure, each Mn ion is octahedrally coordinated by O ions as in the perovskites, leading to the expectation of similar crystal field splittings, particularly a Mn $3d$ t_{2g} manifold below the e_g manifold. In an ionic model, $Tl_2Mn_2O_7$, contains only Mn^{4+} ions. This would result in a fully occupied majority spin t_{2g} manifold, with unoccupied e_g and minority spin t_{2g} states, exactly as in $CaMnO_3$. This provides no plausible DEX mechanism. Subramanian *et al.*¹³ find no evidence for O deficiency, which could provide an alternate doping mechanism. Nonetheless, the ground state is observed to be ferromagnetic¹⁴ and metallic, and even more surprising a CMR effect similar to the perovskites is observed. CMR has also been observed in the In doped material, $(Tl,In)_2Mn_2O_7$.¹⁵

METHOD AND STRUCTURE

This paper reports the results of LSDA calculations of the electronic structure and some magnetic properties of $Tl_2Mn_2O_7$ using the linearized augmented plane wave (LAPW) method^{16,17} with local orbital extensions.¹⁸ The calculations used a basis consisting of more than 2550 functions and a Brillouin zone sampling of 60 special k points in the irreducible wedge. Core states were treated relativistically, while all scalar relativistic corrections were included for the valence states. No shape approximations were made to the density or potential. This is important for open structures with low site symmetries like pyrochlore. The main result is that in the ferromagnetic ground state, the electronic structure near the E_F is very strongly spin differentiated, as was found in the perovskite CMR materials.^{7,10} The mechanism is, however, quite different, and arises from an unexpected, highly itinerant minority spin state associated with the Tl-O ions in the pyrochlore structure.

As mentioned, the Mn ions in $\text{Tl}_2\text{Mn}_2\text{O}_7$ are octahedrally coordinated by O ions (denoted O2). The resulting octahedra are arranged in an fcc crystal structure ($Fd\bar{3}m$, No. 227) sharing common vertices. The Mn-O-Mn bond angles are approximately 134° rather than the 180° of perovskite. This is less favorable for Mn-O-Mn hopping and may be expected to lead to narrower less itinerant bands. The Mn arrangement (four per primitive unit cell) consists of corner sharing tetrahedra, rather than the simple cubic perovskite lattice. This leads to a structure dominated by three membered rings so that antiferromagnetic interactions, if present, will be strongly frustrated. The Tl ions lie on a similar lattice, shifted by $a/2$ along 111, and coordinated by the O2 atoms comprising the Mn-O octahedra and additional O atoms (denoted O1), which are approximately 0.3 \AA closer to the Tl than the O2 atoms.

The experimental crystal structure of Subramanian *et al.*¹³ was used. This structure has a Mn-O bond length of 1.90 \AA , with no evidence of a Jahn-Teller distortion of the octahedra. While consistent with the non-Jahn-Teller Mn^{4+} ions in this material, this is notable in view of the relationship of CMR and structural effects in the perovskites.^{19,20}

ELECTRONIC AND MAGNETIC STRUCTURE

Self-consistent calculations for ferromagnetic $\text{Tl}_2\text{Mn}_2\text{O}_7$ lead to a high spin state with a spin moment of $2.96\mu_B$ per Mn ion. However, as in the perovskites, this is not a pure Mn moment. The spin moment within a 2.0 a.u. radius Mn LAPW sphere is $2.6\mu_B$. A reduction of this order also occurs in the ferromagnetic perovskites, and in that case is due to hybridization with O $2p$ states, which account for much of the “missing” polarization. However, the missing polarization is found in a remarkable location in $\text{Tl}_2\text{Mn}_2\text{O}_7$. The O2 spheres (radius 1.55 a.u.) comprising the octahedra that coordinate the Mn ions contain a negligible polarization of only $0.006\mu_B$ each. In contrast the O1 oxygen spheres (radius 1.55 a.u.), which coordinate the Tl ions and are located 4.10 \AA from the nearest Mn ion account for a polarization of $0.16\mu_B$ each. Each 2.15 a.u. Tl sphere contributes $0.045 \mu_B$.

As mentioned, antiferromagnetic interactions between neighboring Mn atoms cannot be fully satisfied in the pyrochlore structure because of the presence of three membered nearest neighbor Mn rings. Accordingly, calculations were performed for an artificial ferrimagnetic cell in which one of the four Mn spins was flipped relative to the other three in order to investigate the possibility of antiferromagnetic interactions. The flipped Mn has six neighboring Mn of opposite spin, while the other Mn atoms have two neighbors of the opposite spin and four of the same spin. This metastable configuration was found to have an energy 0.033 eV per Mn atom higher than the ferromagnetic state, implying that the Mn-Mn interactions are in fact ferromagnetic consistent with experiment. The total spin moment of this ferrimagnetic unit cell is $5.94\mu_B$, which is very close to what would be obtained assuming Hund’s rule ions. However, as in the ferromagnetic case the polarization inside the Mn spheres is considerably lower, $-2.46\mu_B$ inside the LAPW sphere of the flipped Mn and $2.55\mu_B$ in each of the other three Mn. The stability of the Mn moments when flipped is similar to that noted previously in the perovskites¹⁰ and implies a state for a

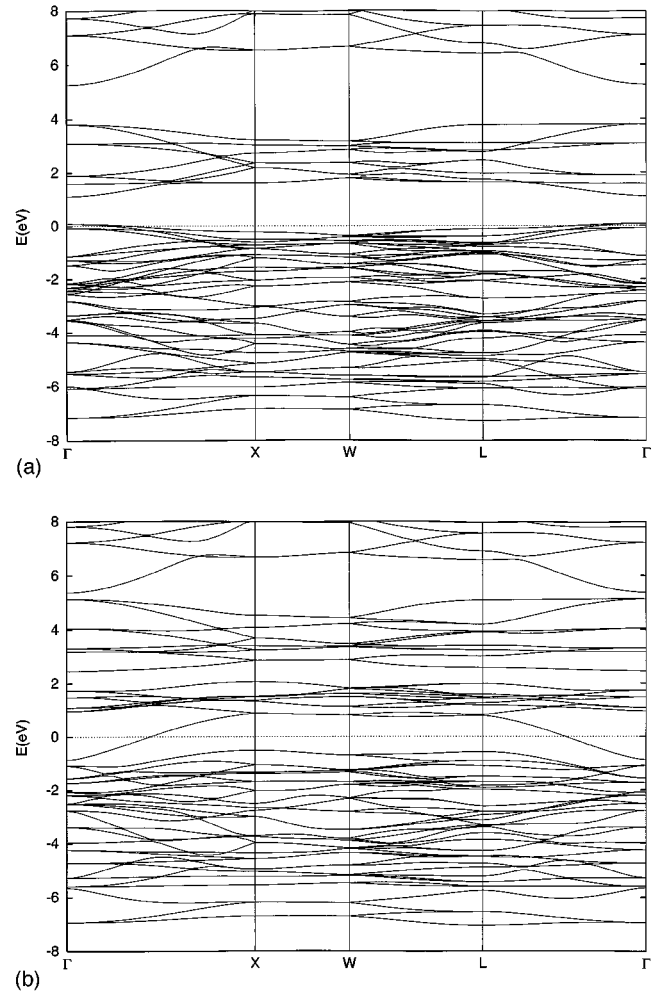


FIG. 1. Majority (top) and minority (bottom) spin band structures of $\text{Tl}_2\text{Mn}_2\text{O}_7$. The Fermi energy is denoted by the dotted horizontal line at 0 eV . The O $2s$ and Tl $5d$ bands are below the lowest bands shown.

substantial temperature range above the Curie temperature in which the Mn moments remain intact but their directions become disordered. The O1 and average Tl polarizations in the ferrimagnetic cell are $0.08\mu_B$ and $0.03\mu_B$, respectively, so that these sites contribute almost the same proportion of the total spin magnetization as in the ferromagnetic case. The projections of the DOS onto the Mn sites are similar to those of the ferromagnetic cell, with the exception that the peak from -7 to -6 eV is suppressed and shifted to lower binding energy with a resulting narrowing of the valence DOS. This peak consists of bonding combinations of O, Mn, and Tl states.

The unexpected Tl and O1 polarization may be understood in terms of the band structure, shown in Fig. 1. The corresponding electronic density of states (DOS) is shown in Fig. 2. The majority spin DOS shows a manifold of primarily O $2p$ states extending from -7 eV to E_F . The Mn majority t_{2g} states are concentrated in the upper part of this manifold from about -2 eV to E_F , while the next 12 bands extending from 1.2 to 3.6 eV above E_F are associated with the Mn e_g and Tl $6s$ states, which are hybridized with O $2p$ states. However, an examination of the projections of the DOS onto the O1 and Tl spheres (Fig. 3) also shows an unexpected

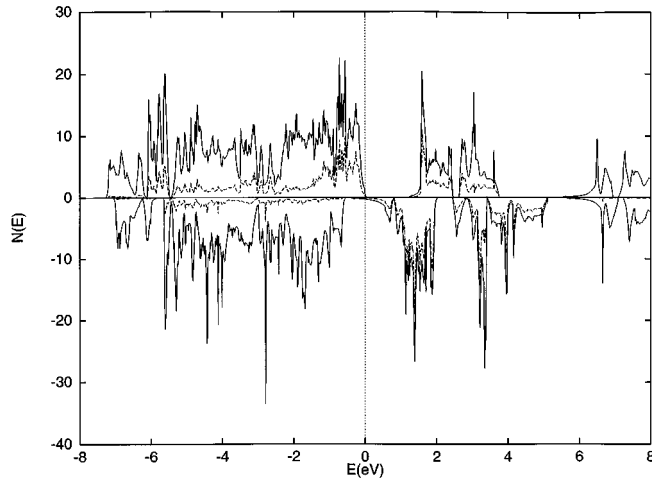


FIG. 2. Electronic DOS (eV^{-1}) of ferromagnetic $\text{Ti}_2\text{Mn}_2\text{O}_7$. The Fermi energy is at zero. The solid lines above (below) zero are the majority (minority) spin total DOS on a per unit cell basis. The dashed lines are the d -like projections onto the four Mn spheres in the cell.

mixing of Ti and O $2p$ states both above and below E_F . This strong Ti-O1 covalency distinguishes $\text{Ti}_2\text{Mn}_2\text{O}_7$ from the perovskites, where the A (La,Ca) site cation donates charge to the active Mn-O bands, but otherwise is inactive in the valence electronic structure. Further, the Ti-O2 distance, while approximately 0.3 \AA longer than the Ti-O1 distance, is still short enough at 2.46 \AA to allow hybridization of the Ti-O1 states with the Mn-O2 states, particularly since below E_F these bands occur in the same energy region, i.e., not surprisingly the O1 $2p$ and O2 $2p$ DOS are both concentrated between -7 eV and E_F . The mixing of these states is responsible for the spin polarization on the Ti and O1 atoms.

In both $\text{Ti}_2\text{Mn}_2\text{O}_7$ and the CMR perovskites, the Mn-O hybridization is spin dependent. In both cases, majority spin Mn t_{2g} orbitals overlap the O $2p$ states and hybridize strongly with them, while the minority spin states, which are shifted by an exchange splitting of about 3 eV lie well above the O $2p$ manifold and hybridize much more weakly (note

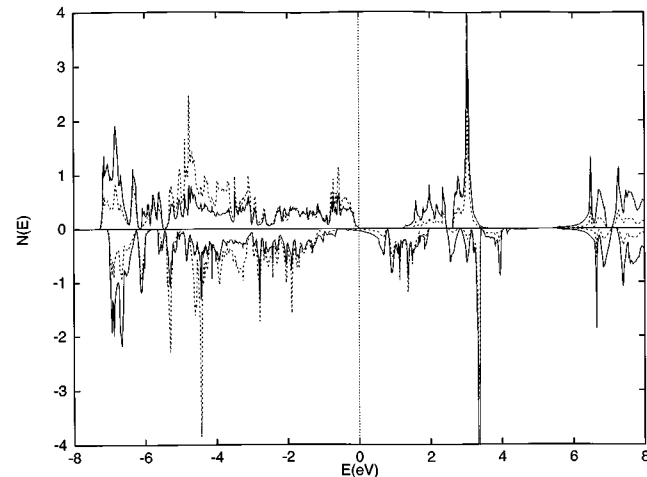


FIG. 3. Projection of the DOS onto the four Ti spheres (solid lines) and p -like character on the two O1 spheres (dashed lines) as in Fig. 2.

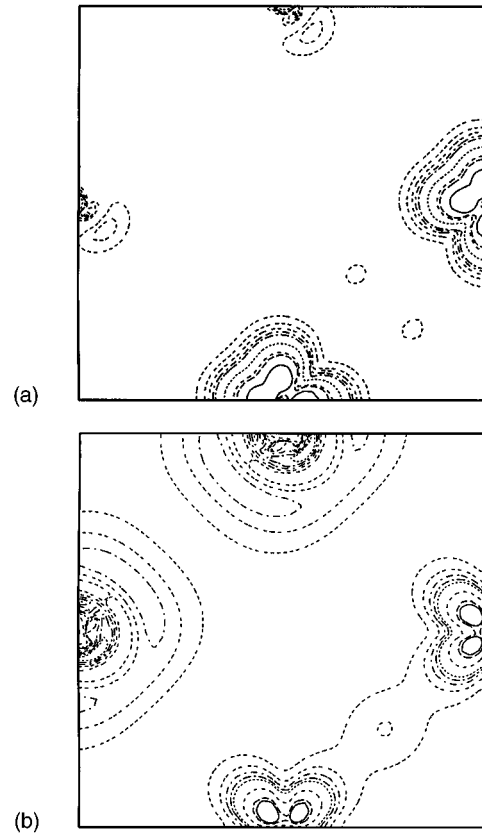


FIG. 4. The top (bottom) panel is a contour plot in a (001) plane of the charge density ($\varphi^*\varphi$) associated with the majority (minority) states at E_F . Ti atoms are at the center of the left and top edges, while Mn are on the bottom and right edges. The first five contour levels are spaced by 0.0004 e/a.u.^3 , the next four by 0.002 e/a.u.^3 , and the final contour is at 0.02 e/a.u.^3 .

that the exchange splitting depends strongly on the band under consideration). In the ferromagnetic perovskite CMR materials, this leads to large majority spin Fermi surface derived from highly itinerant hybridized Mn $3d$ -O $2p$ states, and only small near band edge minority spin sections, which are likely localized due to disorder in these alloys. By contrast, in $\text{Ti}_2\text{Mn}_2\text{O}_7$ 180° Mn-O-Mn bonds are absent. This leads to narrower bands, so that the majority spin Mn t_{2g} -O $2p$ bands are separated by a gap from the Mn e_g derived bands. As a result, there are only small near band edge Fermi surfaces in the majority spin channel. These are from the three flat (effective masses 1.1 , 1.9 , and $1.9m_e$) majority spin bands, dispersing downwards from Γ across E_F leading to three small Fermi surface sections containing a total of 0.086 holes per unit cell.

As in the perovskites there is a gap in the minority spin channel between the O $2p$ manifold and the Mn d states. However, in $\text{Ti}_2\text{Mn}_2\text{O}_7$, a single highly dispersive band crosses the gap reaching a minimum at the Γ point. The charge density associated with this state (Fig. 4) and projections of the DOS onto various sites show that this state has both strong Ti and O1 character and Mn $3d$ -O2 character. The 0.086 electrons contained in the resulting nearly spherical minority spin Fermi surface would by themselves result in a polarization of the Ti-O1 system opposite to that of the Mn, but as mentioned, the Ti-O1 covalency and mixing with

Mn-O2 states extends through much of the valence band region in both the majority and minority spin channels. The mixing with polarized Mn states causes an exchange splitting of these bands and a net positive polarization on the Tl and O1 sites. However, while such mixing of Mn and Tl states occurs through much of the valence band region, it should be emphasized that the heavy mass majority spin states at E_F do not have this character, but are rather predominantly Mn 3d-O2 in character (Fig. 4).

The presence of this minority spin band leads to a metallic minority spin channel. The minority spin Fermi energy DOS is $N_{\downarrow}(E_F)=0.24 \text{ eV}^{-1}$ with an average Fermi velocity, $v_{\downarrow F}=3.3 \times 10^7 \text{ cm/s}$. The majority spin band edge is only 0.07 eV above E_F which leads to the expectation that disorder may suppress the majority spin conduction. The low Fermi velocity $v_{\uparrow F}=0.6 \times 10^7$ reflects the high band masses, while $N_{\uparrow}(E_F)=1.2 \text{ eV}^{-1}$ is larger than the minority spin DOS and strongly energy dependent. A crude estimate of the spin polarization of the electrical conductivity σ may be made by taking $\sigma \propto N(E_F)v_F^2$ (Ref. 21), yielding a rather large $\sigma_{\downarrow}/\sigma_{\uparrow}=6$. This may be an underestimate due to the proximity to the majority band edge, which would lead to an even larger spin differentiation. In any case, the large spin polarization in the transport is consistent with the observation of large magnetoresistance effects near the ordering temperature analogous to heterogeneous magnetoresistive materials such as granular Co-Cu.^{22,23}

SUMMARY AND CONCLUSIONS

Pyrochlore structure $\text{Tl}_2\text{Mn}_2\text{O}_7$ has been studied using LSDA calculations. A ferromagnetic ground state and a magnetization consistent with experiment are found. Similar to perovskite materials showing CMR effects, a large spin differentiation of the band structure at E_F is found. Domain walls between oppositely aligned regions will have a high

resistivity since the itinerant minority spin electrons will have to spin flip to enter the itinerant minority spin states on the other side. One possible explanation for CMR in this case supposes that the state near the Curie temperature consists of randomly oriented domainlike regions of aligned spins having internal electronic structures similar to the ferromagnetic state. If the boundaries between these regions make a large contribution to the resistivity due to the differentiation of the spin up and spin down electronic structures then CMR may result. The origin of the spin differentiation of the Fermi energy electronic structure in $\text{Tl}_2\text{Mn}_2\text{O}_7$ is, however, quite different from the spin dependent Mn-O hybridization and resulting metallic majority spin channel in the perovskites. In $\text{Tl}_2\text{Mn}_2\text{O}_7$ the spin differentiation arises from a highly itinerant Tl-O-Mn derived band at E_F in the minority spin channel. The possibility of Tl covalency is not entirely unanticipated given the crystal chemistry of Tl ions coordinated by O. For example, among the high temperature superconductors a weaker but related covalency is found in $\text{Tl}_2\text{Ba}_2\text{CuO}_6$, where Tl-O covalency causes doping of the cuprate planes even though this is a "clean" nearly stoichiometric material.²⁴ The involvement of Tl states in the electronic structure of $\text{Tl}_2\text{Mn}_2\text{O}_7$ near E_F should lead to stronger spin orbit induced spin flip scattering than in the CMR perovskites. In the above scenario this suggests that very high magnetoresistances may be more difficult to achieve in $\text{Tl}_2\text{Mn}_2\text{O}_7$ relative to the perovskite CMR materials.

ACKNOWLEDGMENTS

Work at the Naval Research Laboratory is supported by the Office of Naval Research. Computations were performed using the NAVO and ARSC facilities under the auspices of DoD HPCMO. I am grateful to Warren E. Pickett for helpful discussions.

-
- ¹R. von Helmolt, J. Wecker, B. Holzapfel, L. Schultz, and K. Samwer, *Phys. Rev. Lett.* **71**, 2331 (1993).
²S. Jin, H. M. O'Bryan, T. H. Tiefel, M. McCormack, R. A. Fastnacht, R. Ramesh, and L. H. Chen, *Science* **264**, 413 (1994).
³G. H. Jonker and J. H. van Santen, *Physica* **16**, 337 (1950); J. H. van Santen and G. H. Jonker, *ibid.* **16**, 599 (1950).
⁴C. W. Searle and S. T. Wang, *Can. J. Phys.* **48**, 2023 (1970).
⁵E. O. Wollan and W. C. Koehler, *Phys. Rev.* **100**, 545 (1955).
⁶C. Zener, *Phys. Rev.* **82**, 403 (1951).
⁷W. E. Pickett and D. J. Singh, *Europhys. Lett.* **32**, 759 (1995).
⁸D. D. Sarma, N. Shanthi, S. R. Barman, N. Hamada, H. Sawada, and K. Terakura, *Phys. Rev. Lett.* **75**, 1126 (1995).
⁹I. Solovyev, N. Hamada, and K. Terakura, *Phys. Rev. Lett.* **76**, 4825 (1996).
¹⁰W. E. Pickett and D. J. Singh, *Phys. Rev. B* **53**, 1146 (1996).
¹¹S. Satpathy, Z. S. Popovic, and F. R. Vukajlovic, *Phys. Rev. Lett.* **76**, 960 (1996).
¹²Y. Shimakawa, Y. Kubo, and T. Manako, *Nature* **379**, 53 (1996).
¹³M. A. Subramanian, B. H. Toby, A. P. Ramirez, W. J. Marshall, A. W. Sleight, and G. H. Kwei, *Science* **273**, 81 (1996).
¹⁴N. P. Raju, J. E. Greedan, and M. A. Subramanian, *Phys. Rev. B* **49**, 1086 (1994).
¹⁵S. W. Cheong, H. Y. Hwang, B. Batlogg, and L. W. Rupp, Jr., *Solid State Commun.* **98**, 163 (1996).
¹⁶O. K. Andersen, *Phys. Rev. B* **12**, 3060 (1975).
¹⁷D. J. Singh, *Planewaves Pseudopotentials and the LAPW Method* (Kluwer, Boston, 1994), and references therein.
¹⁸D. Singh, *Phys. Rev. B* **43**, 6388 (1991).
¹⁹A. J. Millis, P. B. Littlewood, and B. I. Shraiman, *Phys. Rev. Lett.* **74**, 5144 (1995).
²⁰H. Roder, J. Zhang, and A. R. Bishop, *Phys. Rev. Lett.* **76**, 1356 (1996).
²¹P. B. Allen, W. E. Pickett, and H. Krakauer, *Phys. Rev. B* **37**, 7482 (1988).
²²A. E. Berkowitz, J. R. Mitchell, M. J. Carey, A. P. Young, S. Zhang, F. E. Spada, F. T. Parker, A. Hutten, and G. Thomas, *Phys. Rev. Lett.* **68**, 3745 (1992).
²³J. Q. Xiao, J. S. Jiang, and C. L. Chien, *Phys. Rev. Lett.* **68**, 3749 (1992).
²⁴D. J. Singh and W. E. Pickett, *Physica C* **203**, 193 (1992).